

Proximity networks and epidemics

Zoltán Toroczka^{a,b,*}, Hasan Guclu^b

^a*Department of Physics, University of Notre Dame, 225 Nieuwland Science Hall, Notre Dame, IN 46556, USA*

^b*Center for Nonlinear Studies, Theoretical Division, MS B258, Los Alamos National Laboratory, Los Alamos, NM 87545, USA*

Available online 29 December 2006

Abstract

Disease spread in most biological populations requires the proximity of agents. In populations where the individuals have spatial mobility, the contact graph is generated by the “collision dynamics” of the agents, and thus the evolution of epidemics couples directly to the spatial dynamics of the population. We first briefly review the properties and the methodology of an agent-based simulation (EPISIMS) to model disease spread in realistic urban dynamic contact networks. Using the data generated by this simulation, we introduce the notion of dynamic proximity networks which takes into account the relevant time-scales for disease spread: contact duration, infectivity period, and rate of contact creation. This approach promises to be a good candidate for a unified treatment of epidemic types that are driven by agent collision dynamics. In particular, using a simple model, we show that it can account for the observed qualitative differences between the degree distributions of contact graphs of diseases with short infectivity period (such as air-transmitted diseases) or long infectivity periods (such as HIV).

© 2006 Elsevier B.V. All rights reserved.

Keywords: Epidemics; Social networks; Spatial dynamics; Agent-based modeling; Scale-free network

1. Introduction

Epidemics is the disease of the crowds. It is the process where a certain state of an individual is transferred to other individuals by transport through a medium connecting the agents such that eventually a finite fraction of the total population possesses that state. In particular, if that state is an infectious illness, epidemics can have major negative consequences on a population, and thus the development of prevention and mitigation methods gain a crucial importance. In order to develop efficient strategies for prevention and mitigation, however, one must understand the process of disease spread for the particular population in question. There has been considerable work devoted in the past to the so-called compartmentalized models [1–4] where the individuals are assigned one of the finite number of compartments corresponding to their health state (such as susceptible, infected, and recovered/removed) combined with a uniform mixing model for the disease transfer process for the individuals within each compartment. The fate of epidemics in this framework is described by a set of coupled ordinary differential equations. While such an approach is capable of producing reliable

*Corresponding author. Department of Physics, University of Notre Dame, 225 Nieuwland Science Hall, Notre Dame, IN 46556, USA.

E-mail address: z.t@nd.edu (Z. Toroczka).

URL: <http://cnls.lanl.gov/~toro>.

high-level predictions for some diseases (such as influenza) it cannot provide detailed information about non-aggregate variables, which is crucial for developing efficient targeted vaccination and quarantine strategies. Most recently, however, there has been considerable effort invested [5–9] in agent-based or individual-based approaches which build in-silico microscopic models of the population along with its dynamics. After a statistical validation with real data, the agent-based framework is then used as a test-bed for a number of different scenarios for epidemics spread and some of the possible vaccination and quarantine strategies. Although this can be a useful tool for aiding decision making, it is much less amenable to theoretical analysis, the simulation itself being a complex system in its own right. Essentially, an agent-based model is a learning system [22] whose structure and parameters are set such that it reproduces the statistics of real world data. Through the generalizing power of this system then one hopes to gain reliable insight into data-scarce regions of the phase space. Since the level of detail in agent-based modeling can be arbitrarily high, this approach, however, has the promise of giving specific, high-resolution answers to questions like: “Does vaccinating teachers and children between ages 2 and 12 have more impact on slowing disease spread than vaccinating cashiers? Which buildings should be closed in order to stop disease spread?”, etc. To understand the sensitivities in an agent-system for disease spread, and perhaps draw some more general conclusions, one has to build minimalist models for analyzing the data produced by such large-scale simulations. This paper presents a simple framework for understanding some of the topological features of dynamic disease contact graphs, using data produced by a particular agent-based simulation, EPISIM [5–7,10], developed at Los Alamos National Laboratory (LANL).

In this article we shall confine ourselves to the case where disease is transferred through a *contact process* between two individuals. Here contact is understood in a fairly loose sense, only requiring that the two individuals be in the spatial proximity of each other. The proximity distance required for disease spread is certainly disease dependent, ranging from actual physical contact (such as in the case of sexually transmitted diseases) through a couple of feet to confinement in a building with common ventilation system (airborne diseases).

Another aspect that we will be considering is the *mobility* of agents. In contrast with, for example, the spread of viruses on computer networks which can be considered as a flow process on a static structure, most populations are composed of mobile agents. As a result, the contact network resulting from the “collision dynamics” of the agents is itself a dynamic entity. This is especially an important aspect for human populations in dense urban areas. Currently, urbanization is in an explosive stage [11]: the number of megacities (with over ten million inhabitants) is estimated to increase from 14 in 1995 to 21 cities by 2015. By 2030 it is estimated [11] that over 60% of the world’s population will live in cities. For example, the population of São Paulo (Brazil), the world’s third most populated city, has grown from a population of 265,000 to 18 million in the last 100 years. Almost half of São Paulo’s inhabitants were not born there [11]. Large cities act like “magnets” for people living in rural areas or smaller cities (especially true in Third World countries), since over half of the gross domestic product in most countries is made of industrial and commercial activities taking place in these cities [11], and thus they represent hopes for prosperity. A recent mathematical model of aggregation accounting for this effect was introduced by Leyvraz and Redner [12]. Under such circumstances the problem of disease spread, due to the dense nature of the contact fabric among people in cities, becomes of real concern.

In the following we present a brief description of agent-based modeling using EPISIM as an example. We recall some of the topological properties of the contact network obtained by this simulation for the case of Portland, OR. The key observation that we will be addressing in this paper refers to the connectivity distribution of the people–people contact graph which seems to be rather different from other measurements of contact graphs such as the sexual contact network measured by Liljeros et al. [13,14]. We will then propose a framework that can account for these differences in a unifying manner. We conclude by discussions on the limitation of the model and possible extensions.

2. An agent-based approach to epidemics

The transportation analysis and simulation system (TRANSIMS) [15–19] developed at LANL is an agent-based, cellular-automata model of traffic in a particular urban area (the first model was for Portland, OR,

USA). TRANSIMS decomposes the transportation planning task using three different time-scales. A large time-scale associated with land use and demographic distribution is employed to create activities for travelers (activity categories such as work, shopping, entertainment, school, etc.). Activity information typically consists of requests that travelers be at a certain location at a specified time, and includes information on travel modes available to the traveler. This is achieved by creating a synthetic population and endowing it with demographics matching the joint distributions given in the US census data. The synthetic households are built by also using survey data from several thousands of households, which are observations made on the daily activity patterns of each individual in the household. These activity patterns are associated with synthetic households with similar demographics. The locations are estimated taking into account observed land use patterns, travel times, and transportation costs. The intermediate time-scale assigns routes and trip chains to satisfy the activity requests. This is done by feeding the estimated locations into a routing algorithm to find minimum cost paths through the transportation infrastructure consistent with constraints on mode choice [18,19]. The third and shortest time-scale is associated with the actual execution of trip plans in the road network. This is done by a cellular automata simulation [16,17] through a detailed representation of the urban transportation network. The simulation resolves the traffic induced when everyone tries to execute their plans simultaneously resolving distances down to 7.5 m and times down to 1 s. It provides an updated estimate of time-dependent travel times for each edge in the network, including the effects of congestion, which it feeds then to the router and location estimation algorithms, which produce new plans. This feedback process continues iteratively until it converges to a quasi-steady state in which no one can find a better path in the context of everyone else's decisions. The resulting traffic patterns compare well to observed traffic. The entire process estimates the demand on a transportation network using census data, land usage data, and activity surveys. More information and including availability of the software can be obtained from Ref. [15].

EPISIM [5–7,10] is actually one of the applications of TRANSIM and it is built on top of that. Diseases such as colds, flu, smallpox, or SARS are transmitted through air between two agents, if they spend long enough time in the proximity of each other, or in building with closed air ventilation. This means that we can assume that the majority of the infections will take place in locations, like offices, shopping malls, entertainment centers, mass transit units (metros, trams, etc.). Thus, by tracking the people in our TRANSIMS virtual city, we can generate a bi-partite contact network, or graph, formed by two types of nodes, namely people nodes and locations nodes. In the case of Portland, there are about 1.6 million people nodes and 181,000 location nodes and over 6 million edges between them. These are huge graphs, representing considerable challenges for the measurement of their properties.

Let us denote by L the set of locations and by P the set of people. The people and locations are indexed by integers, called *person-id* and *location-id*. The vertex set of a graph G will be referred to as $V(G)$ while the edge set will be referred to as $E(G)$. The degree of a vertex $v \in V(G)$ is the number of edges incident on v . The activities in the EpiSIMs graphs have a time-periodic character. However, on average, people typically resume their activity patterns after 24 h and thus graphs corresponding to different week-days are similar to one another. The time labels to be defined below are measured time intervals for a duration of 24 h and the graphs defined also refer to this 24 h period. The temporally resolved bi-partite graph of people and locations is denoted as (G_{PL}, β) , where the only edges present are between individuals and the locations they visit. The vertex set is defined as $V(G_{PL}) = P \cup L$. An edge $e \in E(G_{PL})$ is defined by the ordered pair (p, l) where $p \in P$ is the person-id of the individual and $l \in L$ is the location-id of the location which it visited. $\beta(e)$ signifies a time label associated with the edge $e \in E(G_{PL})$, and it is defined as the set of non-overlapping time intervals $\beta(e) = \beta(p, l) = \{I^{(1)}(e), I^{(2)}(e), \dots\}$, given by $I^{(j)}(e) = I^{(j)}(p, l) = [t_{in}^{(j)}(e), t_{out}^{(j)}(e)]$ between the “in-time” $t_{in}^{(j)}$ and “out-time” $t_{out}^{(j)}$ to and from l of p . The reason for a number of different time intervals is that the same person can visit several times the same location during a day (such as office–lunch–office, etc.). If two intervals $I(e)$ and $I(e')$ are non-overlapping, then we define $I(e) < I(e')$, iff $t_{out}(e) \leq t_{in}(e')$. We consider two other types of contact networks: the *people–people* graph, denoted by (G_P, π) , and the *location–location* graph, (G_L, λ) . In G_P , an individual $u \in P$ is represented by one vertex. There is an edge $e = (u, v) \in E(G_P)$ if the individuals $u, v \in P$ have come into contact, i.e., if $\exists e_u, e_v \in E(G_{PL})$ and $l \in L$, such that $e_u = (u, l)$, $e_v = (v, l)$ and $\beta(e_u) \cap \beta(e_v) \neq \emptyset$. The time label associated with this edge therefore is calculated by $\pi(e) = \bigcup_{l \in L} \beta(e_u) \cap \beta(e_v)$, composed of intervals of time when they have *shared* the same location (any) during a day.

The location–location graph (G_L, λ) is a *directed graph*, where every vertex represents a location from L , and a directed edge $\mathbf{e} \in E(G_L)$ is defined by the *ordered pair* $\mathbf{e} = (k, l)$, $k, l \in L$, if there is at least one person $p \in P$ going from k to l anytime during the day, see for an example Fig. 1. Naturally, since a person can be in a single location at a given time instant, $\beta(p, k) \cap \beta(p, l) = 0$ ($k \neq l$). Thus $\mathbf{e} = (k, l)$ is an edge from k to l , if $\exists I^{(j)}(p, k) \in \beta(p, k)$ and $I^{(m)}(p, l) \in \beta(p, l)$ such that $I^{(j)}(p, k) < I^{(m)}(p, l)$ and for $\forall I(p, n) \in \beta(p, n)$ with $\forall n \in L \setminus \{k, l\}$, either $I(p, n) < I^{(j)}(p, k)$ or $I^{(m)}(p, l) < I(p, n)$. An entrance time of p at l coming from k is obviously $t_{in}^{(m)}(p, l)$. Since this is a continuous time, discrete event process, these entrance times into location l of people coming directly from location k during a day, can be ordered into a set $\lambda(k, l) = \lambda(\mathbf{e})$, which forms the *weight label* of edge \mathbf{e} in $E(G_L)$. We are interested in entrance times to a location because this way we are able to record when an infection enters a location and thus the time after which possible infections can occur for people visiting that location. Fig. 2 shows the measured degree distribution of the people–people contact graph G_p keeping only those edges which come from time-stamp overlaps of at least 1 h. As one can see, the degree distribution has an exponential cut-off (at about $k = 700$) and a peak, not reminiscent of pure power-law (scale-free) networks. Although the curve seems to have power-law behavior portions of it, nothing really can be concluded based on this data, since this behavior is only about over one decade. The exponential cut-off is a must, because an individual cannot be in contact with $O(N)$ other people during a day. The graph integration interpretation that we will present in the next section, however, identifies some key ingredients that might be responsible for the shape of this distribution.

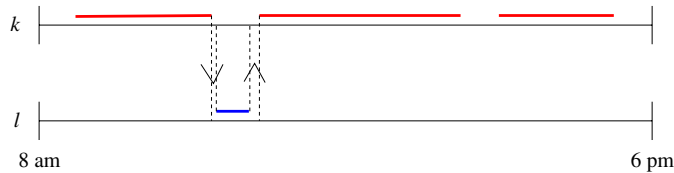


Fig. 1. An example for how directed edges are defined in the location–location graph: k and l denote two locations, k is an office while l is a nearby cafe. The horizontal axis is time and the thick lines denote the presence of a person p at that location. This diagram could stand for: p was at k during mid-morning hours, then it went to l for lunch, then back to k and then somewhere else (to doctor’s appointment) then back to k then somewhere else, etc.

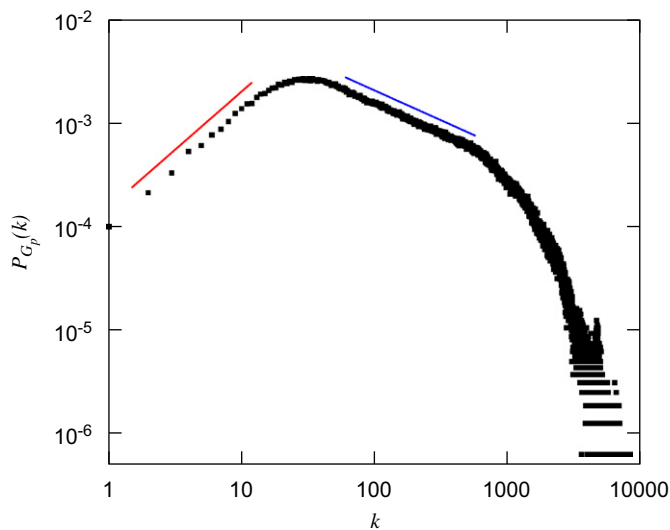


Fig. 2. Degree distribution of the people–people contact network G_p (see text for definition) in EPISIM Oregon data. The measurement of the degree distribution is done on a single instance of the G_p (and thus G_{pL}) graph. The contact time threshold used was 1 h. There are 5788 points in the data set and $k_{max} = 8368$. The slopes of the straight lines are 1.13 and -0.58 , respectively.

3. Proximity networks

Some of the most difficult questions in epidemics concern the spatio-temporal dynamics, as opposed to looking at disease spread as a percolation process on fixed structures. Ref. [20] is a most recent attempt studying epidemics as a branching process building effective contact graphs with scale-free and small-world behavior. This paper illustrates that the details of the dynamics can have drastic effects on disease spread by creating contact graphs with heterogeneous structures.

As we have seen from the EpiSim example above, the true contact graph is a dynamic structure with temporal behavior that can be encoded as time-stamps associated with edges. If one neglects the time-stamps, the graph obtained is the *maximum* contact graph, showing which individuals came in contact at all, during a day. On the other hand, at every instant, the graph of contacts is a set of disconnected small graph clusters showing which individuals are in contact *right at that moment*. Naturally, the maximum contact graph is much denser than the instantaneous contact graphs. Due to the mobility of the individuals, the contacts are changing, and if one would like to know who was in contact with whom over a period of time, we need to *integrate* or *collapse* the instantaneous contact graphs in that time period. If our goal is to produce an *effective* contact graph for a particular disease, so that the disease spread can be treated as a flow process on this effective graph, we need to collapse the instantaneous contact graphs over the typical infectivity period of an individual. For the sake of brevity, we shall refer to the effective integrated contact graph as the *proximity network* of the disease. In case of aerial-born diseases like SARS and smallpox, the infectivity period is on the order of several days, while for some sexually transmitted diseases, like HIV, it is much longer, and can be on the order of years. In the former case, the maximum degree of a node is relatively small (constant compared to the system size) bounded by the number of contacts an agent can possibly make in a short period of time (days), whereas in the latter case the number of accumulated contacts (and thus the number of possibly infected people) can be very large. In this latter case is when we expect to have scale-free behavior for the degree distribution of the contact graph. Indeed, several measurements on the distribution of sexual interactions in human populations [13,14] seem to confirm this expectation. In the remainder of this article we show a very simple model for proximity networks which can capture some of these observations, in particular the scale-free character.

Let us denote the instantaneous contact graph at instant t by $G(t)$. The time-integrated graph or *proximity graph* $\bar{G}(T)$ is given by the union of all edges of the instantaneous graphs from time 0 to time T . In other words, if $\mathbf{A}(t) = \{a_{ij}(t)\}$ is the adjacency matrix of $G(t)$, the adjacency matrix $\bar{\mathbf{A}}(T)$ of $\bar{G}(T)$ is given by

$$\bar{a}_{ij}(T) = \bigvee_{t=0}^{t=T} a_{ij}(t), \quad (1)$$

where $a \vee b = 0$ if and only if $a = 0$ and $b = 0$, otherwise $a \vee b = 1$, $a, b \in \{0, 1\}$. The dynamics of the integrated network is determined by the dynamics of the contact making process between pairs of agents i and j . Depending on the nature of the potentially disease-transmitting contacts, the matrix elements $a_{ij}(t)$ might be subject to “exclusion constraints”. For example, in the case of sexual contacts, the instantaneous graphs are made of a collection of dimers and/or isolated nodes. This induces the constraint $\sum_{j, j \neq i} a_{ij} \leq 1$, $i = 1, \dots, N$ on the matrix elements of $G(t)$. For diseases spread by air, the transmission usually happens in locations which have a limited capacity. Assuming that all agents within a location can be infected if at least one of them is infectious (for example, due to shared ventilation system), the contact graph within a location is a clique. The constraints imposed on the instantaneous adjacency matrix $\mathbf{A}(t)$ can be thus be formulated as

$$(1 - a_{ik})a_{ij}a_{jk} = 0 \quad \text{for all } i, j, k \in 1, \dots, N, \quad (2)$$

$$\sum_{j, j \neq i} a_{ij} \leq K \quad \text{for all } i \in 1, \dots, N, \quad (3)$$

where K is the maximum clique size (maximum location capacity). The first of these equations is a necessary and sufficient condition for a graph to be the disjoint union of cliques and the second limits the size of the cliques to K . Eq. (2) expresses the fact that all connected triplets must form a triangle (if i and j are connected

and j and k are connected, then i and k are connected as well—transitivity). In the physics network literature, the alternative formulation of the same condition is that the clustering coefficient of $G(t)$ is unitary.

Here we will not consider a full theory of dynamic proximity networks, that will be developed elsewhere. Instead, we introduce the most simplistic model of network growth which still reproduces the qualitative features of the observations in the beginning of this section.

The probability $\bar{p}_{ij}(T)$ that nodes i and j are connected in the proximity graph at time T increases for larger values of T . Assuming a uniform link generation picture, the probability that in the next step a potentially disease-spreading connection/contact takes place between agents i and j is written as $\rho g_i g_j$ where the weight g_i quantifies the “gregariousness” of agent i , its propensity to generate new links. Note that this model does not explicitly resolve the exclusion constraints (2)–(3). One can think of the parameter ρ effectively incorporating the spatial information, which should be resolved in spatial models for contact dynamics. The probability that after T steps nodes i and j are connected is given by

$$\bar{p}_{ij}(T) = 1 - (1 - \rho g_i g_j)^T, \quad T \geq 1. \quad (4)$$

The parenthesis in (4) represents the probability of nodes i and j *not* connecting in one step, and its T th power is for non-connection during all steps. One minus this probability is obviously the connection probability during any of the steps $1, 2, \dots, T$. According to this, highly gregarious people will more likely be connected to each other than less gregarious. They will also get connected earlier than others. ρ is a parameter which makes $\rho g_i g_j \leq 1$, but at this point is a free parameter. If we want to stay close to the claim that in one step a node does not accumulate more links than it is allowed by the exclusion conditions, we need to consider ρ to be a small number. If all nodes have the same gregariousness parameter g then we recover a growing binomial random graph model and the degree distribution of the proximity graph will always stay a Poisson distribution with a parameter that grows exponentially with time until the graph becomes a complete graph. This is certainly expected, given that there is no heterogeneity in the mixing among agents.

There are certainly many possible, more realistic extensions to our model, in particular making the gregariousness coefficients time dependent and taking into account more explicitly the exclusion constraints. Time-dependent gregariousness coefficients would correspond to cases where, for example, there is an increasing cost of adding a link (because it involves traveling further away) or the health state of the agent (e.g., infected or not) can modify their ability to generate new links. Here we will only study the case where these coefficients are time-independent.

Under what conditions for the gregariousness distribution of a population will we observe power-law (scale-free) degree distributions for its proximity network? One expects that populations where all individuals have similar gregariousness values, no power law should be observed for the degree distribution of $\bar{G}(T)$, whereas heterogeneous distributions for g_i would likely generate distributions with a power-law regime in them. The expected degree of node i in $\bar{G}(T)$ is

$$\bar{d}_i(T) = \sum_{j=1}^N \bar{p}_{ij}(T) = \sum_{j=1}^N [1 - (1 - \rho g_i g_j)^T]. \quad (5)$$

For small ρ , $\rho T \ll 1$, this is simply $\bar{d}_i(T) \simeq \rho T (\sum_j g_j) g_i$, i.e., it is directly proportional to its gregariousness coefficient. This certainly makes sense in a social context since more gregarious people will have on average more contacts than others. In this limit (small ρ , and not too large T values, such that $\rho T \ll 1$), our model is similar to the Chung Lu model [21] of random power-law graphs with expected degree sequences. The difference is that in our case the g_i 's are random variables drawn independently from a given distribution, while in the Chung Lu model the node weights are prescribed functions of their index. In the small ρ limit initially the graph will form disconnected clusters, but it does not strictly obey the exclusion conditions. As time goes on the links accumulate on the proximity network and one can obtain a regime where, depending on the gregariousness distribution, scale-free contact networks emerge. If the agents are not removed from the system, but keep accumulating contacts, eventually a finite network will reach the complete graph limit and stop there. If the infectivity period is finite, however, the network will reach a steady-state structure characteristic to the population dynamics and the disease. This might be scale-free, homogeneous, or anything in between.

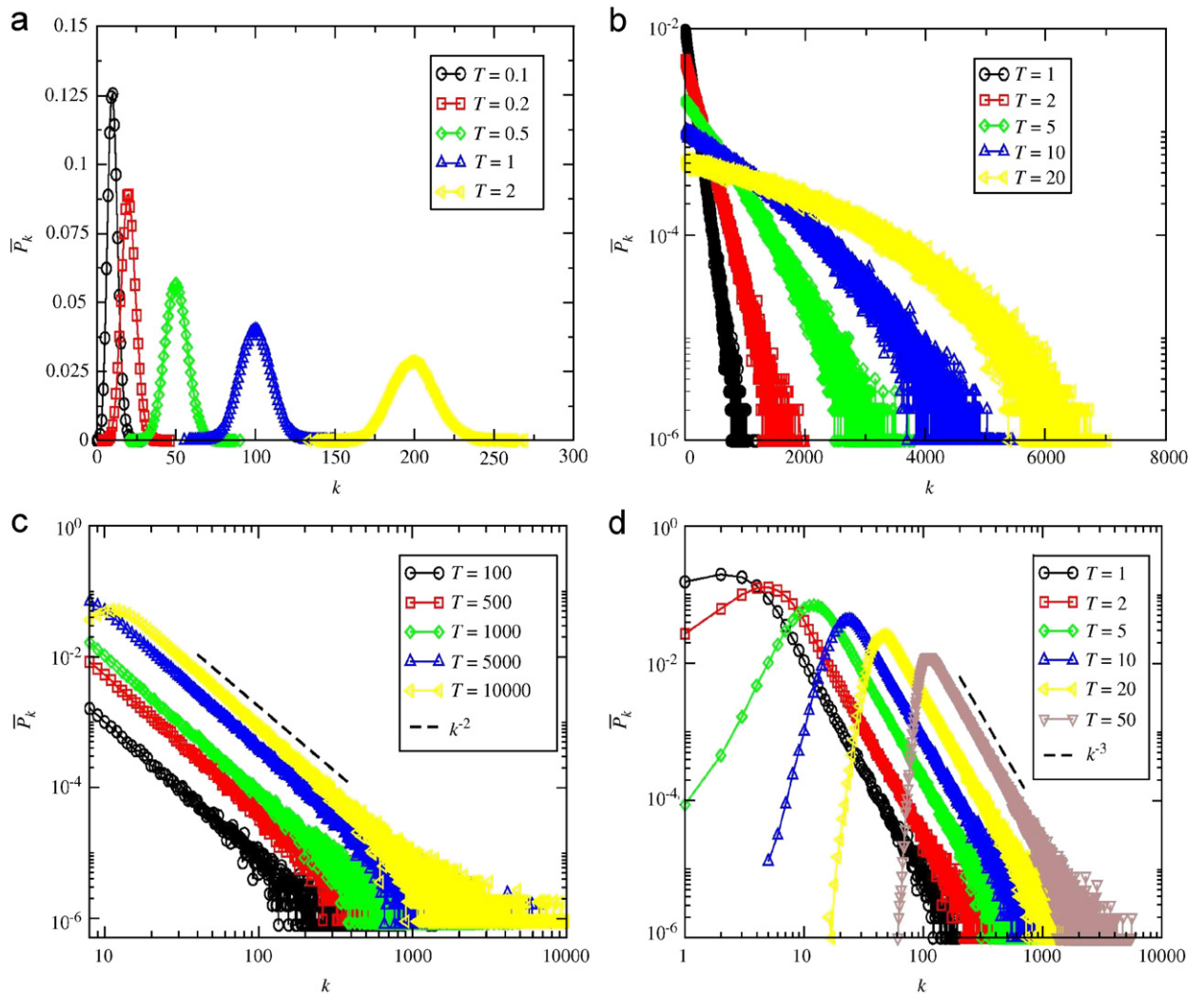


Fig. 3. Degree distributions of the proximity network for various distributions of the gregariousness: (a) constant g ; (b) exponential distribution for g ; (c) and (d) power-law g . All networks have $N = 10^4$ nodes.

Going back to the EPISIM contact network data we notice that this simplistic model reproduces (see Fig. 3) qualitatively some of the key features shown in Fig. 2. Although the EPISIM distribution has a sharp, exponential cut-off, it shows a tendency of forming a power-law tail before the cut-off just as in our model. In addition, it seems that the low- k tail shows a similar power-law tendency, also in qualitative accordance with the data generated by our simplistic model, see Fig. 3d. With this model one can also generate distributions (not shown) with small (including sub-unitary) exponents for the power-law regime followed by a sharp cut-off, matching closer the case of Fig. 2.

4. Conclusions

We presented the basis of a framework to account for the dynamics of contacts in epidemic processes, through the notion of dynamic proximity graphs. By varying the integration time-parameter T , which is the period of infectivity, one can give a simple account for some of the differences in the observed contact networks for different diseases, such as smallpox or AIDS. Our simplistic model also seems to shed

some light on the shape of the degree distribution of the measured people–people contact network from the EPISIM data.

We certainly do not claim that the simplistic graph integration model (4) above is a good model for dynamic contact graphs. It only contains the essential ingredients for such processes to produce a qualitative agreement with some observations. We expect that further refinements and extensions to this picture, in particular deriving the link probabilities in the dynamic proximity graph from more realistic contact dynamics should improve the agreement between models and data.

Acknowledgments

The authors thank for support DOE W-7405-ENG-36, and S. Eubank, for useful discussions and availability of data.

References

- [1] J.D. Murray, *Mathematical Biology II*, third ed., Springer, Berlin, 2004.
- [2] L. Edelstein-Keshet, *Mathematical Models in Biology*, SIAM, Philadelphia, PA, 2005.
- [3] F. Bauer, C. Castillo-Chávez, *Mathematical Models in Population Biology and Epidemiology*, Springer, Berlin, 2001.
- [4] R.M. Anderson, R.M. May, *Infectious Diseases in Humans*, Oxford University Press, Oxford, 1992.
- [5] G. Chowell, J.M. Hyman, S. Eubank, C. Castillo-Chávez, *Phys. Rev. E* 68 (2003) 066102.
- [6] S. Eubank, H. Guclu, V.S. Anil Kumar, M.V. Marathe, A. Srinivasan, Z. Toroczkai, N. Wang, *Nature* 429 (2004) 180.
- [7] C. Barrett, S. Eubank, M. Marathe, in: D. Goldin, S.A. Smolka, P. Wegner (Eds.), *Interactive Computing: A New Paradigm*, Springer, Berlin, 2006, pp. 353.
- [8] S. Riley, N.M. Ferguson, *Proc. Nat. Acad. Sci. USA* 103 (2006) 12637.
- [9] V. Colizza, A. Barrat, M. Barthelemy, A. Vespignani, *Proc. Nat. Acad. Sci. USA* 103 (2006) 2015.
- [10] C. Barrett, S. Eubank, M. Marathe, H. Mortveit, A. Srinivasan, N. Wang, *Proceedings of the 15th Annual ACM-SIAM Symposium on Discrete Algorithms*, New Orleans, 2004, p. 718.
- [11] E. Zwingle, *Cities*, *Natl. Geogr. Mag.* 202 (2002) 70–99.
- [12] F. Leyvraz, S. Redner, *Phys. Rev. Lett.* 88 (2002) 068301.
- [13] F. Liljeros, C.R. Edling, L.A.N. Amaral, H.E. Stanley, *Nature* 411 (2001) 907.
- [14] R.M. Anderson, R.M. May, *Nature* 333 (1988) 514.
- [15] (<http://transims.tsasa.lanl.gov>), (<http://www.transims.net>).
- [16] K. Nagel, *Phys. Rev. E* 53 (1996) 4655.
- [17] K. Nagel, P. Stretz, M. Pieck, S. Leckey, R. Donnelly, C.L. Barrett, Technical Report LA-UR-97-3530, 1997.
- [18] C.L. Barrett, R. Jacob, M.V. Marathe, *SIAM J. Comp.* 30 (2001) 809.
- [19] C. Barrett, K. Bisset, R. Jacob, G. Konjevod, M. V. Marathe, in: *Proceedings of the European Symposium on Algorithms*, Lecture Notes in Computer Science, vol. 126, Springer, Berlin, 2002.
- [20] A. Vazquez, *Phys. Rev. Lett.* 96 (2006) 038702.
- [21] F. Chung Graham, L. Lu, *Ann. Combinatorics* 6 (2002) 125.
- [22] N. Gilbert et al., *JASSS* 9(2) (2006), <http://jasss.soc.surrey.ac.uk/9/2/9.html>.